Design and Integration of a High-Resolution Multispectral Optical Payload for Next-Generation Earth Observation Missions

Giovanni Bianucci, Andreas Findeis, Federico Fiorenzoli, Gabriele Grisoni,
Umberto Papa, Ronan Rodrigues, Massimiliano Rossi, Fabio E. Zocchi
Media Lario S.r.l.
Bosisio Parini, Italy
massimiliano.rossi@medialario.com

***Abstract*—This paper reports the design, manufacturing, and integration of an optical multispectral payload for Earth observation, capable of achieving high spatial resolution with a Ground Sampling Distance (GSD) of less than 1 meter. The payload is designed to meet the stringent requirements of modern Earth observation missions, providing high-precision multispectral imagery for applications in urban planning, environmental monitoring, and disaster management.**

The optical system incorporates a corrected Ritchey Chrétien telescope design with aspheric optics to achieve high performance across visible and near-infrared bands. A compact and lightweight Carbon Fiber Reinforced Polymer (CFRP) structure, optimized through extensive thermal and structural analysis, ensures operational stability under the harsh conditions of space. The payload integrates state-of-the-art multispectral detectors with optimized bandpass filters for high spectral fidelity and radiometric accuracy.

The manufacturing phase focused on precision polishing, optical alignment, and meticulous metrology to ensure compliance with the sub-micron tolerances required for high-resolution imaging. The P/L test plan includes rigorous vibration, thermal-vacuum, and optical performance validation to simulate launch and on-orbit conditions confirming its capability to deliver high-quality multispectral data with sub-meter resolution.

This work highlights the challenges and solutions in developing next-generation optical payloads, emphasizing design innovations, manufacturing precision, and robust integration methodologies. The payload is poised to contribute to Earth observation missions, offering unparalleled detail and versatility for commercial applications.

Keywords — Very High Resolution, Earth Observation, Multispectral, Optical Sensors.

I. Introduction

In recent years, the demand for high-resolution Earth observation data has surged, driven by the growing need for precise, timely, and multispectral information across a wide range of applications. From urban planning and environmental monitoring to natural disaster response and agricultural assessment, modern remote sensing missions increasingly require payloads capable of delivering detailed imagery with both spatial and spectral fidelity.

The IRIDE programme [1], involving the creation of six satellite constellations for total of over 60 satellites, is promoted by the Italian Government, developed with funds from the National Recovery and Resilience Plan (PNRR), and coordinated by ESA with the support of the Italian Space Agency. IRIDE aims to establish a comprehensive space-based infrastructure for environmental monitoring, security, and scientific research. Within this framework, the IRIDE VHR1 (Very High Resolution 1) satellite, developed by Thales Alenia Space in partnership with Media Lario and TSD Space represents the optical component of the constellation specifically engineered to deliver very high spatial resolution imagery with rapid revisit capabilities.

IRIDE VHR1 is equipped with a high-performance optical payload optimized for sub-meter ground sampling distance (GSD) in the panchromatic band and multi-spectral imaging with high radiometric accuracy. The platform design emphasizes agility, enabling fast slew maneuvers and off-nadir imaging up to large angles to ensure frequent access over areas of interest. VHR1 operates in a sun-synchronous LEO orbit (SSO) balancing spatial resolution and swath. At the heart of the system is a corrected Ritchey-Chrétien telescope, enhanced with aspheric optics to ensure consistent imaging performance across the field of view. The structural assembly utilizes Zerodur mirrors and CFRP components, selected and optimized through detailed thermal and structural analysis to ensure dimensional stability under launch and on-orbit conditions.

The payload incorporates a high-performance multispectral detector with custom bandpass filters engineered for accurate spectral discrimination. The manufacturing process emphasizes ultra-precise polishing, alignment, and metrology to meet sub-micron-level tolerances, which are critical for achieving the desired image quality. To ensure flight readiness, a comprehensive test and validation campaign will be executed, including vibration, thermal-vacuum, and optical performance assessments. These tests emulate launch stresses and spaceborne thermal conditions, thereby confirming the payload's capability to deliver reliable, high-quality data in operational settings.

The following sections detail the system architecture, its thermal design, manufacturing and integration activities, and the results of the laboratory test campaign on the Electro Optical Model representative of many features of the upcoming Structural Thermal Model (STM) and Proto Flight model (PFM).

By addressing the technical challenges involved in realizing a compact, high-resolution multispectral payload, this development contributes to the ongoing advancement of next-generation Earth observation platforms.

TABLE I. VHR MAIN SPECIFICATIONS

Parameter	Specification	Notes
Ground Sampling Distance	0.92 m (PAN) 3.68 m (RGB-VNIR)	@ nadir
Focal length	3.5 m	
Aperture	0.34 m	
Payload mass	≤ 25 kg	
Pixel sizes	7 µm PAN 28 µm RGB-NIR	
Bands	Pan: 450 – 800 nm MS 1: 450 – 520 nm MS 2: 520 – 590 nm MS 3: 630 – 690 nm MS 4: 770 – 890 nm	
SNR for each band	≥ 100 PAN ≥ 140-177 MS	With on-board TDI
Swath width	> 11 km	@ nadir
Along track stripe	Up to 1200 km	
Dynamic range	12 bit per pixel	

II. SYSTEM ARCHITECTURE

The Payload main specifications are reported in Table I and the layout of the optical design is provided in Figure 1 showing the Ritchey-Chrétien (RC) configuration [2], a widely used design in astronomical and Earth observation instruments where high image quality over a wide field of view is required.

The system consists of a 340 mm concave hyperbolic primary mirror and a convex hyperbolic secondary mirror. The primary mirror captures incoming light and reflects it toward the secondary mirror, which then focuses the light on the focal plane. A set of additional 6 lenses act as a field corrector to minimize residual aberrations (mainly field curvature and astigmatism) and to maintain high imaging quality across a wide field covering the 84 mm detector.

Multiple colored ray bundles represent different field angles (off-axis points), showing that the design provides good off-axis performance — a hallmark of RC telescopes. The RC design naturally eliminates coma and spherical aberration, leaving only astigmatism and field curvature as dominant residual aberrations, which are minimized here by the corrective optics.

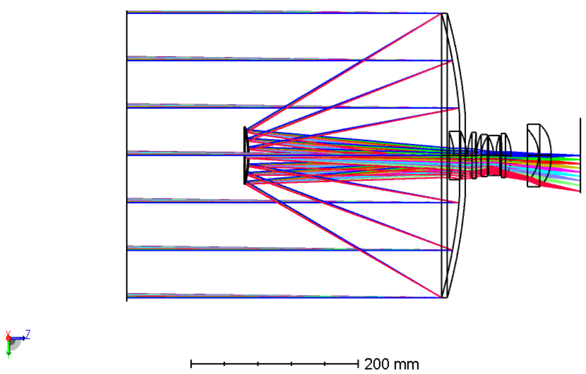

Fig. 1. Optical Lay-out of the IRIDE VHR1 telescope.

The telescope mirrors polished by Media Lario are made of Zerodur low-thermal expansion glass mounted on a stable CFRP structure to minimize thermal distortions in the operational environment. These optics feature a protected Silver coating extensively qualified and used for institutional as well commercial missions. The field corrector lenses instead are made of radiation hardened glasses properly selected to reduce chromatic aberration.

The IRIDE VHR1 system integrates the Teledyne ORBIS IC-49 12K detector on its custom focal plane assembly (FPA), developed by TSD Space together with the Payload Electronics able to drive the FPA and configure image acquisition. The ORBIS 49 is a high-performance, space-qualified sensor that combines charge domain TDI CCD with CMOS on a single chip, offering best of both technologies to deliver high sensitivity, low noise, and fast readout rates, that are critical for achieving both high spatial resolution and efficient multi-band data acquisition in orbit. The ORBIS 49 is characterized by:

- Large Active Area: Supporting very high-resolution imaging with small pixel sizes (7 µm), enabling sub-meter ground GSD.
- High Dynamic Range: Allows the sensor to accurately capture scenes with a wide range of reflectance levels, from dark surfaces to highly reflective ones (such as snow or clouds) via TDI operation.
- Low Noise and High Linearity: Critical for ensuring precise radiometric measurements across the entire field of view.
- Radiation Tolerance: Designed to maintain performance over extended missions in Low Earth Orbit.

In-field spectral separation is employed to capture multiple spectral bands. The detector area is physically divided into separate regions, each coated, at wafer level, with narrowband optical filters corresponding to specific spectral ranges (e.g., Blue, Green, Red, Near-Infrared). As the satellite moves forward along its orbit (push broom scanning), each point on the ground is imaged simultaneously in different spectral bands. Each line of pixels along the track corresponds to a strip of the Earth's surface in a specific wavelength. Because all bands are captured essentially at the same time, this method avoids temporal misalignments between bands, a crucial advantage for high-accuracy multispectral analysis (e.g., vegetation indices, water quality monitoring).

III. THERMAL DESIGN

The external allocation on the NIMBUS platform, depicted in Figure 2, is a rather challenging configuration to keep the payload’s temperatures within the desired 20 ± 5 °C operational range. In order to ensure a proper image quality, the thermal design heavily relies on Multi-Layer Insulation (MLI) blankets (shown in yellow in the picture). These blankets radiatively insulate the payload from the space environment and also shield a radiator (purple in the picture), adopted to dissipate the FPA heat loads, from the spacecraft. Additionally, insulating washers are used to conductively separate the payload from the platform's top plate.

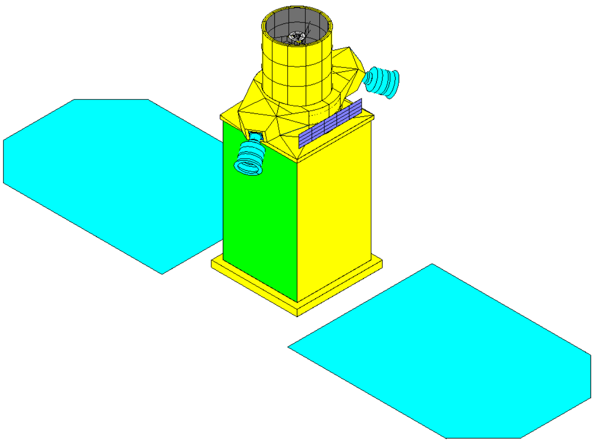

Fig. 2. ESATAN thermal model of the IRIDE VHR1 satellite

The thermal control strategy follows a cold-biased design approach, ensuring that the payload remains slightly colder than required under the hottest expected conditions. This enables the use of heaters to adjust the temperature to optimal conditions during image acquisition. The heaters are capable of maintaining the unit above the minimum required temperatures during the coldest conditions with an average power consumption of 22 W per orbit in the predicted worst case. All heater lines, except those on the CFRP mainframe, operate on an on/off basis, with switch-on and switch-off set points managed by the satellite.

The central CFRP tube is designed with a specific thermo-optical configuration. The surfaces exposed to the optical cavity are painted black for stray-light control, while areas covered by insulating blankets are coated with low emissivity materials to further insulate the structural mainframe. This design is crucial because the temperature difference between the mainframe and the Assembly Integration and Testing (AIT) temperature of 20 °C is the primary factor affecting the imaging performance. By controlling the temperature set points of the baseplate heaters, the average temperature of the CFRP plate can be regulated, minimizing thermal distortions on the primary mirror.

The thermal architecture is therefore built on the following principles:

- Use of MLI blankets to thermally insulate the payload from the environment.
- Very low Coefficient of Thermal Expansion (CTE) for sensitive opto-mechanical components, such as mirrors and the CFRP structure.
- A radiator for dissipating internal heat to deep space, supporting a cold-biased thermal approach.
- Heaters and sensors to regulate the temperature of the optical assembly.

The Thermal Control System (TCS) has been designed to meet the mission profile conditions and was optimized based on several key assumptions regarding the satellite controller and load cases:

- A baseline control threshold of ± 0.5 °C during imaging;
- Maximum average power consumption of 22 W;
- Maximum of 1.2 million on/off cycles over the 5-year mission, equating to a maximum of 40 cycles per orbit;
- Four operational cases, based on the worst cold and worst hot conditions;
- A significant reduction in the variation of the M1-M2 distance keeping it within ± 0.5 µm.

Despite the efficiency of the achieved TCS design, it is expected that once in orbit, the CFRP tube will shrink slightly due to moisture release and, as the optical design is particularly sensitive to the M1-M2 distance, the Modulation Transfer Function (MTF) will progressively decrease, potentially rendering the telescope inoperable. To counter balance this effect, an in-orbit thermal refocusing capability has been implemented. Not only this adjustment will compensate for CFRP shrinkage caused by moisture release in vacuum, but it will also potentially correct any mismatches between the thermal model predictions and actual conditions without further challenging the TCS consumptions.

In-orbit MTF measurements, conducted as part of the Calibration and Validation (Cal/Val) procedure, contracted to Planetek Italia, will determine the optimal refocusing position. Once optimal MTF performance is achieved, the refocusing system will be maintained during observations at a constant temperature for the mission's lifetime, as the CFRP tube will have stabilized to its final dimension. The refocusing procedure will be performed during the commissioning phase but can be repeated during the mission if necessary. However, real-time refocusing for thermal control is not planned. The TCS will neutralize thermal induced changes by ensuring the CFRP tube remains close to 20 °C thanks to the closed-loop feedback coming from the several sensors installed on the system.

IV. Manufacturing and Integration

Mirror manufacturing involves a precise, multi-step process. Unlike spherical mirrors, which have a consistent radius of curvature, aspherical mirrors feature complex, non-spherical surfaces that allow for aberration correction in advanced optical systems. Transforming a raw blank into a high-precision aspheric optic requires several key stages: grinding, acid etching, polishing, and coating.

Using computer-controlled machinery and diamond-embedded tools, material is carefully removed from the mirror blank to form both a lightweight backside structure and the aspheric contour of the optical surface. This is an iterative process, employing progressively finer abrasive grits to closely approach the desired aspheric shape. While grinding defines the general geometry, the resulting surface remains too rough for optical use.

Following grinding, acid etching is performed to mitigate subsurface damage caused during the previous phase. This chemical milling method selectively removes material by controlling the etchant's composition and exposure time, preventing micro-cracks while maintaining tight control over dimensional and interface characteristics.

Because standard acid etching would degrade the precision-ground aspheric profile, a targeted approach to subsurface damage removal is used specifically for the optical area. In this phase, polishing is applied to glass parts to uniformly remove surface material, preventing micro-cracks and further reducing grinding marks and surface waviness.

The critical polishing stage is mandatory to achieve a smooth surface meeting functional requirements. In this time-intensive process proprietary techniques developed by Media Lario for Zerodur mirrors are adopted. For complex aspheric surfaces, computer-controlled polishing with bonnet tools are used, offering exceptional control over material removal and enabling nanometer-level surface accuracy. Interferometry with Computer Generated Holograms (CGH) is essential at this stage, providing real-time feedback on surface form and guiding corrections to meet tight specifications.

The final process step is coating, which imparts the mirror's reflective properties. A thin layer of high-reflectivity Silver is applied using vacuum deposition methods like thermal evaporation or magnetron sputtering. This coating enhances reflectivity and overall system throughput, thereby improving the telescope's signal-to-noise performance. A completed primary mirror is shown in Figure 3.

Similar manufacturing techniques are employed for the field corrector lenses, with the primary distinction being the use of anti-reflective coatings rather than reflective ones. These coatings are tailored to maximize optical throughput and minimize stray light and ghosting effects.

The six lenses, comprising both spherical and aspherical shapes, are polished and integrated into a single, tightly-toleranced subassembly: the field corrector. The decision to pre-assemble the field corrector, supported by a thorough sensitivity analysis performed during the design phase in Zemax OpticStudio, simplifies the integration procedure limiting the number of optical elements to be assembled into the telescope and therefore reducing the overall duration of the system alignment.

To reduce risk in the integration of the IRIDE STM and PFM, the program's model philosophy includes a simplified Electro Optical Model (EOM). Though simplified, the EOM is representative of key functional aspects of the final telescope. It served as a powerful validation tool, enabling verification of the entire electro-optical system, including imaging performance and the complete image acquisition and processing chain (optics, detector, Focal Plane Assembly, Payload Electronics). Additionally, many of the AIT activities could be performed in advance, allowing refinement of test benches and procedures.

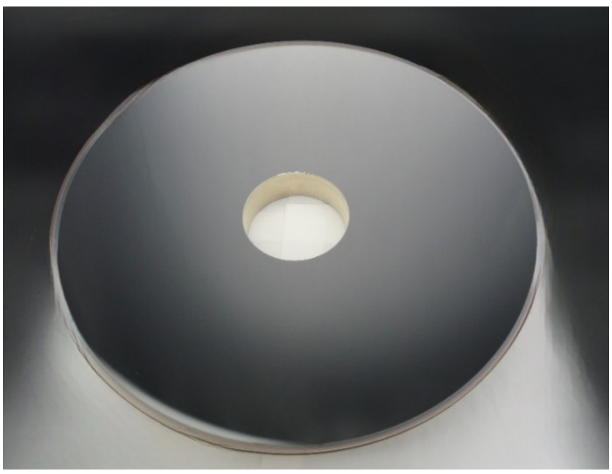

Fig. 3. Coated primary mirror for the IRIDE VHR1 EOM.

The EOM, leveraging on the same mirrors as the STM and PFM, is a Ritchey-Chrétien telescope, a design renowned for its aplanatic performance, assembled with the same stringent requirements valid for the other models. The primary mirror is mounted on a CFRP baseplate, chosen for its high stiffness-to-weight ratio and low thermal expansion, critical for maintaining stability in changing temperatures. The mirror is supported using bipods designed to offer stable support while minimizing stress on the optics.

CFRP structural tube, matched thermally to the baseplate, supports the secondary mirror. Proper alignment of this mirror is essential for high image quality and is achieved through a detailed double-pass interferometric alignment process. This method ensures precise measurement and adjustment of the secondary mirror's position and tilt relative to the primary mirror, securing accurate collimation and minimizing aberrations.

In the final stage, the field corrector, encased in a titanium housing, is integrated into the optical path beneath the baseplate. Its purpose is to expand the field of view and correct for chromatic aberrations. The fully assembled EOM is shown in its handling jig in Figure 4.

V. Engineering Model Results

An extensive testing campaign has been conducted in laboratory conditions on the integrated EOM to verify its optical performance while refining test procedures and facilities in view of the future activities to be run on the STM and PFM models. The telescope met several requirements including mass, wavefront, focal length, field of view, throughput, linearity, in-field stray-light, Signal to Noise Ratio. A detailed report of some of the tests is provided in the next paragraphs specifically MTF, Photo Response Non-Uniformity and the refocusing sub-system.

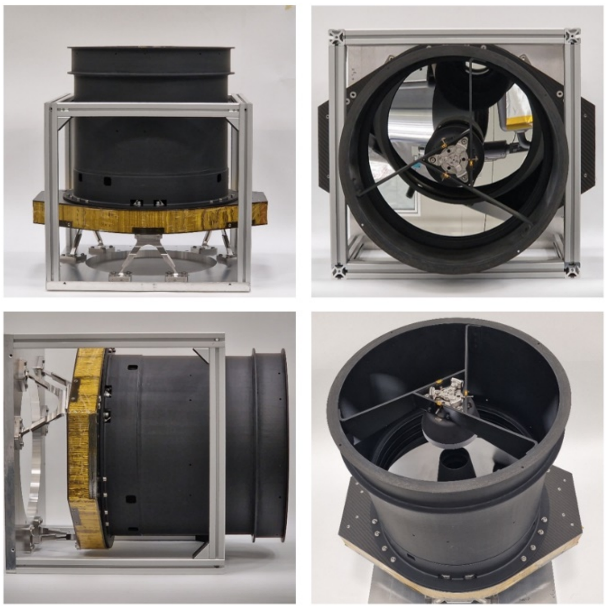

Fig. 4. Integrated EOM unit

A. MTF Results

A slanted edge target in chrome printed on a 1" glass support with 4 squares (2 positive 2 negative) was installed on the focal plane of an F/21 imaging collimator (aligned interferometrically prior to the tests) set-up in front of the IRIDE EOM. The sensor of the payload was progressively shifted by a defined amount along the optical axis and the image of the target was recorded each time. For a given focal plane position, vertical and horizontal MTFs were computed on two perpendicular sides of the target square to detect the best focus of the system. The sequence was then repeated in other locations of the sensor corresponding to different fields of the telescope to identify the best focus plane. This task was achieved by adjusting the fine thread screws integrated into the FPA that are locked in position at the end of the process.

Measured MTFs after optimization are reported for reference in Table II for the 7 µm pixel size PAN1 and Table III for the 28 µm pixel size MS1. Similar results are obtained on PAN2 and the other MS channels. For the high-resolution PAN channels all the horizontal MTFs are nicely meeting requirements while few fields show vertical MTFs out-of-spec. These non compliances are due to a blooming effect that is visible in Figure 4 and that is associated with the adoption in the testing phase of the Area Mode of the sensor to perform vertical MTF calculations, a condition that does not affect the TDI Mode foreseen in flight. The same procedure with a commercial CMOS camera resulted in full compliance demonstrating the quality of the telescope alignment.

TABLE II. MEASURED MTFS FOR PAN1 CHANNEL

Field	Hor. MTF	Vert. MTF	Req.
[°]	*[%]*	*[%]*	*[%]*
-0.6	14 ± 1	12 ± 1	> 11
-0.3	12 ± 1	6 ± 1	> 11
0.0	14 ± 1	12 ± 1	> 11
+0.3	15 ± 1	7 ± 1	> 11
+0.6	14 ± 1	10 ± 1	> 11

TABLE III. MEASURED MTFS FOR MS1 CHANNEL

Field	Hor. MTF	Vert. MTF	Req.
[°]	*[%]*	*[%]*	*[%]*
-0.6	20 ± 1	23 ± 1	> 11
-0.3	31 ± 1	30 ± 1	> 11
0.0	35 ± 1	34 ± 1	> 11
+0.3	32 ± 1	30 ± 1	> 11
+0.6	25 ± 1	28 ± 1	> 11

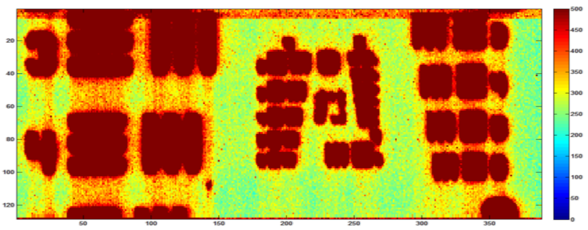

Fig. 5. Contrast enhanced image of a USAF target showing the vertical blooming affecting Area Mode.

B. PRNU

PRNU arises from inherent imperfections in the manufacturing process of image sensors. Even under uniform illumination, each pixel may produce slightly different signal levels due to variations in quantum efficiency, electrical gain, and illumination. While these differences are usually minor, they can introduce significant artifacts when observing subtle surface features or small changes over time. Consequently, an accurate map of the PRNU must be generated and, if necessary, used for either real-time correction or during post-processing.

Testing the PRNU of an optical payload typically involves a carefully controlled laboratory setup that simulates uniform illumination conditions. For the VHR1, Media Lario has adopted a 1 m integrating sphere featuring 10 halogen lamps able to radiate over the PAN and MS bands the necessary illumination with high spatial and angular uniformity across its output port. The device is shown in Figure 5 with its 400 mm outport fully illuminated.

Accurate PRNU testing is not trivial and must account for several potential sources of error including, the integrating sphere itself that must be well-calibrated to ensure that it provides truly uniform radiance across the field of view of the payload as any non-uniformity in the illumination can be mistaken for PRNU.

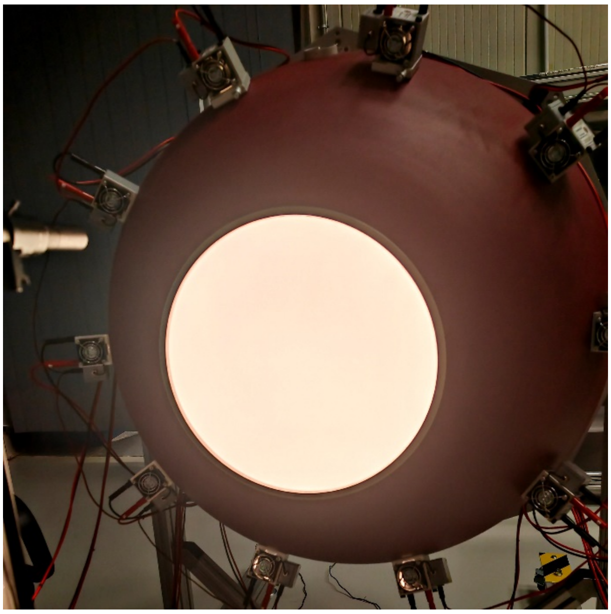

Fig. 6. One meter integrating sphere adopted for the VHR1 calibration.

TABLE IV. MEASURED PRNU FOR THE DIFFERENT CHANNELS

Channel	Measured	Requirement
PAN	0.5 ± 6 %	10.0 %
MS4	0.2 ± 6 %	
MS3	0.2 ± 6 %	
MS2	0.2 ± 6 %	
MS1	0.3 ± 6 %	

PRNU is defined as the standard deviation of the measured intensities from the mean value of the image and is therefore computed as the spatial standard deviation of the photo-response non-uniformity in % from the mean.

Measurements were carried out with the P/L setup in front of the integrating sphere radiating at approximately 50% of the sensor dynamic range for all six channels. PRNU was calculated after calibrating the images with the following procedure:

- A previously acquired dark was subtracted from the raw image (dark acquisitions should be collected in a TVAC set-up covering the whole range of the operational temperatures but for the EOM only a room temperature acquisition was foreseen);
- the resulting array was normalized over a flat image (also subtracted of the same dark);
- intensities were re-scaled to the median value of the raw image;
- dead pixels were removed;
- computation of the PRNU was performed on the residual 2D matrix.

The measured PRNU are reported for each channel in Table IV. Very good calibration levels were obtained even taking into account the (2-sigma) uncertainty potentially affecting the PRNU measurements.

C. *Refocusing sub-system*

The contraction of the CFRP structure caused by the moisture release is considered potentially too high and uncertain to be corrected only by design. Moisture release of the main tube will translate the M2 subsystem towards M1, decreasing their relative distance with a significant impact on the optical performance. Therefore, a thermal mechanism was designed to compensate for the M1-M2 relative distance change.

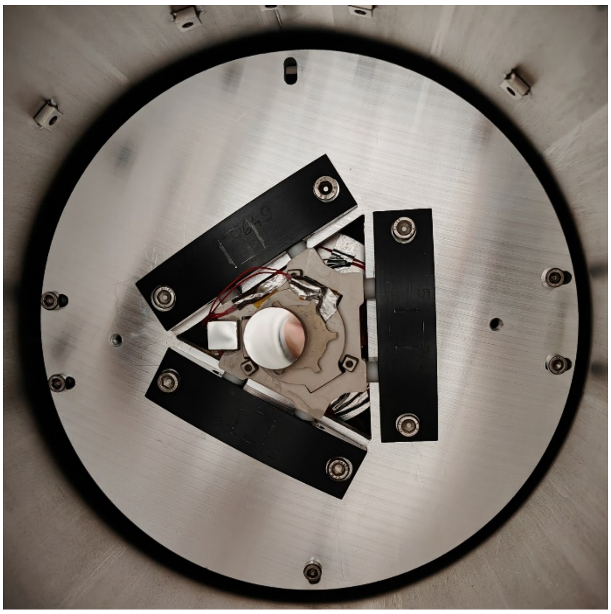

Fig. 7. M2 sub-assy installed in the vacuum chamber with target mirrors.

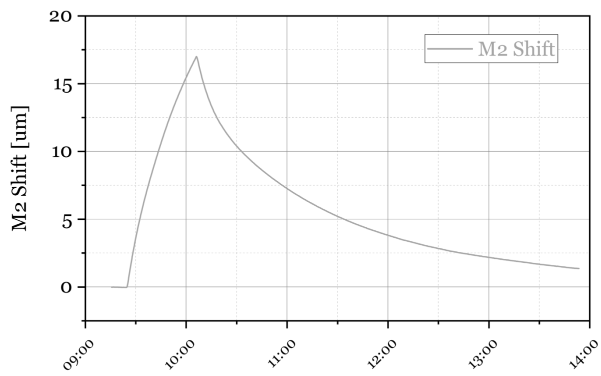

Fig. 8. M2 I/F displacement

A dedicated test on the M2 sub-assy was then carried out with the objective of performing a vacuum test with heaters and sensors to gather more precise data for:

- Displacement of the M2 interface
- Thermal distribution on the sub-system assembly.

The mock-up was fixed coaxially to a small vacuum chamber able to reach 10^{-6} mbar. A two-beam differential interferometer (SIOS DI-5000) was installed outside the viewport of the chamber to monitor the relative displacement of two target mirrors connected respectively to the M2 interface and its fixed mount while heaters were powered up to warm the mechanism between 20 °C and 40 °C. The measured shift between the two mirrors is reported in Figure 7. The total power applied was 2.5 W well in line with the available power in the operational scenario.

The test proofs that the thermal refocusing mechanism proposed for the IRIDE VHR1 can precisely correct the M2 interface position as a result of the heat injected via dedicated heaters. The minimum displacement goal of 12 µm has been achieved and exceeded in all trials.

VI. CONCLUSIONS

The EOM has provided optical and electro-optical validation of the system design generally meeting all relevant optical requirements. The integration of the Pre-EM FPA has been smooth, and it has validated the alignment mechanism. Electro-optical performances are met, particularly the native across track MTF (ACT). As for ALT MTF, it cannot be fully tested in Area Mode due to vertical blooming, an effect not present in the operational TDI mode.

The EOM campaign has optimized most of the AIV procedures that will be adopted for the IRIDE VHR1 STM and PFM models.

ACKNOWLEDGMENT

The authors would like to express their sincere gratitude to all colleagues and collaborators in TAS-I, TSD Space and Planetek who contributed to valuable discussions, technical insights, and constructive feedback throughout the development of this work.

We particularly thank also the ESA team who assisted with critical review the development of the project.

The present work has been caried out under an ESA Contract for the purposes of EO PNRR IRIDE PROGRAMME funded by the European Union through

NextGenerationEU-RFF and by the Presidency of the Council of Ministries of the Italian Republic pursuant to Article 1, paragraph 254, of Law 160/2019' and through the Presidency of the Council of Ministries from the Complementary Fund. Views expressed herein can in no way be taken to reflect the official opinion the European Union/European Commission/ ESA /Presidency of Council of Ministers of the Italian Republic. Views and opinion expressed are those of the author(s) only and the European Union/European Commission/ ESA /Presidency of Council of Ministers of the Italian Republic cannot be held responsible for any use which may be made of the information contained therein.

REFERENCES

[1] G. Costa et al., "IRIDE: The New Italian Space Programme," IGARSS 2024 - 2024 IEEE International Geoscience and Remote Sensing Symposium, Athens, Greece, 2024, pp. 6663-6665, doi: 10.1109/IGARSS53475.2024.10640803.

[2] S. Rosin, ''Ritchey–Chretien Corrector System,'' Appl. Opt., 5, 675–676 (1966).